Received: 3 November 2021 | Revised: 27 January 2022 | Accepted: 9 February 2022

DOI: 10.1002/amp2.10114

REVIEW

JOURNAL OF ADVANCED MANUFACTURING AND PROCESSING WILEY

In-situ curing of 3D printed freestanding thermosets

Chongjie Gao[1] | **Jingjing Qiu**[2] | **Shiren Wang**[1,3]

[1]Department of Industrial and Systems Engineering, Texas A&M University, College Station, Texas, USA

[2]Department of Mechanical Engineering, Texas Tech University, Lubbock, Texas, USA

[3]Department of Materials and Science Engineering, Texas A&M University, College Station, Texas, USA

Correspondence
Shiren Wang, Department of Industrial and Systems Engineering, Texas A&M University, College Station, Texas, USA.
Email: s.wang@tamu.edu

Funding information
National Science Foundation, Grant/Award Numbers: CMMI-1933679, CMMI-1934120

Abstract

Direct-ink-writing (DIW) provides a high-efficiency way for thermoset printing while rapid in-situ curing has a significant role in manufacturing rate, quality, performance, and flexibility. In this review, in-situ curing methods that can be integrated into DIW were discussed, including frontal polymerization, electromagnetic heating, photochemistry, electron beam, and resistance heating curing. The in-situ process monitoring and curing kinetic analysis technologies such as differential scanning calorimetry (DSC), Raman spectroscopy, Fourier transform infrared spectroscopy (FT-IR), broadband dielectric spectroscopy (BDS), ultrasonic dynamic mechanical analysis (UDMA), fluorescence spectroscopy, were briefly presented. The working mechanism and features of these characterization measurements are studied. Furthermore, machine learning and other artificial intelligence tools used for the optimization of printing materials, topology design, printing path, and defect detection sensitivity are reviewed. Finally, some future research directions for the DIW and in-situ curing of thermosets are addressed.

KEYWORDS

direct-ink-writing, in-situ curing, machine learning, real-time monitoring, thermosets

1 | INTRODUCTION

Polymer composite materials have demonstrated lightweight, easy manufacturing, and outstanding mechanical properties.[1–4] Particularly, thermosetting polymer composites have attracted extensive attention due to their chemical and corrosion resistance, thermal and environmental stability, and high mechanical strength. Currently, they have been widely used in the aerospace, automotive, energy, and defense industries.[1,2,5,6] In some scenarios, thermosets are even used to replace metals and ceramics.[2,7] Global thermoset demand is expected to reach $31.7 billion by 2026.[8,9] Emerging additive manufacturing (AM), mainly including 3D printing, is considered as the next-generation manufacturing method of thermosets due to the design flexibility, freeform manufacturing process, reduced lead time, and negligible material waste. There are many additive manufacturing methods available for printing thermosets, such as stereolithography (SLA), digital light processing (DLP), continuous liquid interface production (CLIP), filament fused fabrication (FFF), selective laser sintering, and direct-ink-writing (DIW).[2,8,10–12] Among these approaches, DIW also referred to as robocasting, is an extrusion-based 3D printing technology and provides a high-efficiency way for material printing due to its low cost and versatile capability. DIW has succeeded in printing metals, ceramics, polymers, and even bioactive materials. It can also be applied for 3D printing of wearable individual health monitoring devices and soft robotics.[13–17] Many fillers such as carbon nanotube, carbon fiber, graphene, and metal nanoparticles, can be easily added into the ink for improved properties or multifunctionalities.[2]

Many curing methods for thermosets have been implemented for decades.[18,19] The most popular way to

cure thermosets is to utilize external heat, normally through ovens under vacuum or inlet atmosphere. However, such oven curing needs hours to days of curing, which results in an extensive energy consumption.[20] Therefore, it is difficult to fit in the emerging DIW process since oven curing has to be implemented upon the completion of the printing.[21] In contrast, in-situ curing for thermosets has attracted increasing attention in recent years.[22] The in-situ curing of thermosets is critical for printing precision, final performance, and design/manufacturing flexibility. Many in-situ curing methods for thermosets have been developed. Based on the working principle, these methods can be categorized into three main types, including (1) thermal-induced curing such as resistance, induction, ultrasonic, and microwave, (2) irradiation curing such as infrared, laser electron beam (EB), ultraviolet (UV), X-ray, and γ-ray curing, and (3) exothermic frontal polymerization curing.[1,8,18,23] However, not all the curing methods can be employed for DIW and in-situ curing of thermosets. Although DIW of thermosets has been reported by some literature, it was usually followed by X-ray or γ-ray curing afterward. Based on the working mechanism, these curing methods can also be recategorized into five types, including frontal polymerization, electromagnetic heating, photochemistry, electron beam, and resistance heating curing. The frontal curing is based on the exothermic reaction of frontal polymerization. For the electromagnetic thermal in-situ curing, microwave, laser, and photothermal curing methods are introduced but the thermal additives for photothermal curing are expensive. Electron beam curing is a kind of irradiation method, and the resistance thermal method is based on joule heating. The photochemistry method is the UV curing method which is originally a kind of irradiation method.

The AM process for thermosetting materials starts from the design stage where the computational aided design (CAD) model is developed and converted to g-code before it is imported into a 3D printer to obtain the final product. To get the part with desired performance, various printing parameters need to be optimized. The parameters are often adjusted manually based on the experience of the operators and the working circumstances, which is time-consuming. More importantly, many combinations of the parameters may lead to inconsistency in the printed parts.[24] To figure out those issues, artificial intelligence (AI) such as machine learning (ML) and computer version, has been used to understand the relationship between the performance of the printed thermosets and the process parameters at different stages of the DIW process.[25–27] Though some reviews have reported the machine learning application in the DIW process, most of them have focused on the noncontact DIW, powder bed fusion (PBF), directed energy deposition (DED), and fused filament deposition (FDM).[24,28–30] It is believed that these AI technologies will help build the next-generation smart manufacturing system and accelerate the industry 4.0.[31] Currently, there are three stages that ML technologies can be applied in additive manufacturing: material and topology design, printing parameter optimization, and defect detection, based on a DIW process.

Although there is some literature available about AM processing of thermosetting polymer and composites, almost all of them are focused on the printing methods and resultant performance.[32,33] Some reviews introduced DIW of thermosets, but only focused on the ink preparation.[2] To the best of our knowledge, no literature has been published to provide a systemic review regarding the emerging DIW and in-situ curing of thermosets. In this review, in-situ curing methods for DIW thermosets are categorized into five types: frontal polymerization, electromagnetic heating, resistance heating, electron beam, and photochemistry curing, as shown in Figure 1. The electromagnetic-based thermal curing method includes microwave heating, photothermal, and laser heating curing. The basic working mechanism, advantages, and disadvantages of these in-situ curing methods for DIW thermosets are reviewed and compared. In addition, the in-situ cure monitoring and characterization methods have been reported. To improve the efficiency, performance, and quality of the DIW thermosetting parts, ML is applied in the design, manufacturing, and quality stages. Some other state-of-art technologies, such as computer vision, molecular dynamic (MD) modeling, are also used to optimize the DIW for thermosets. Finally, the research direction and prospect for rapid and costless DIW in-situ cured method for thermoset polymer are listed.

2 | IN-SITU CURING-INTEGRATED DIRECT WRITING

2.1 | Frontal polymerization in-situ cured DIW thermosets

The frontal polymerization-based in-situ curing method for thermosets is a novel curing strategy receiving much attention in recent years. This curing method is based on the frontal curing reaction in which the monomer and the latent initiator are heated as far as the initiator obtains sufficient energy to ignite the self-propagating polymerization reaction.[35,39] The heat would be generated continuously by the polymerization reaction to further sustain the reaction which converts the monomer

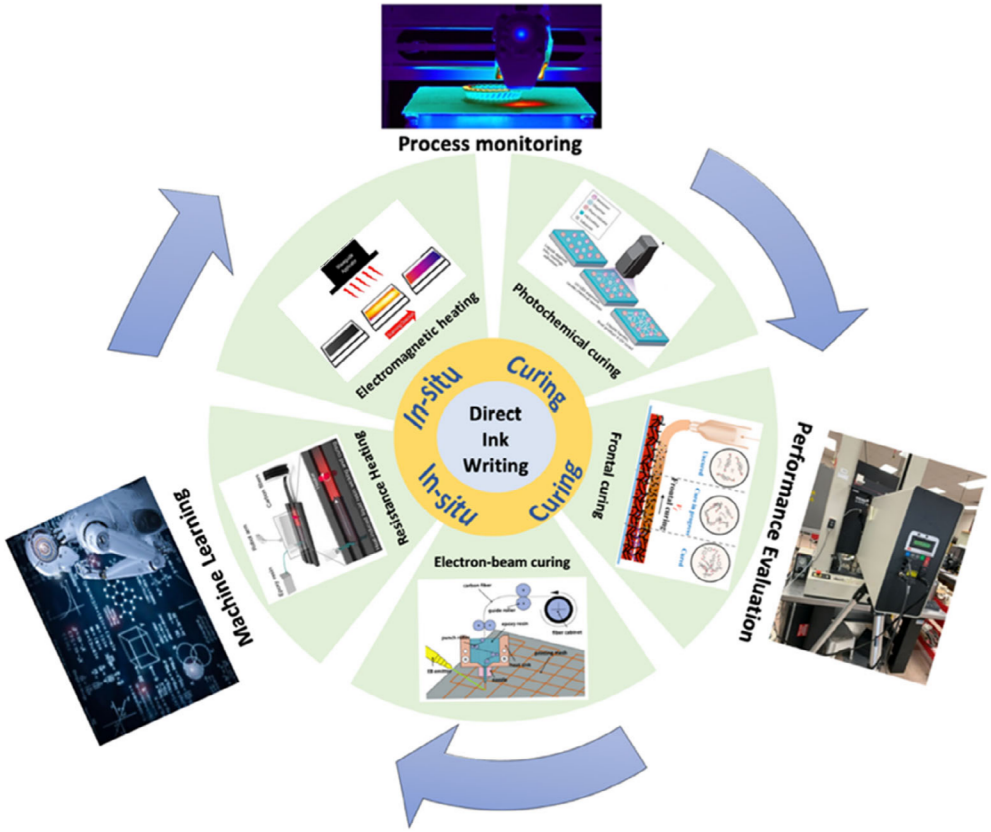

FIGURE 1 The roadmap of DIW and in-situ curing of thermosets[34–38]

into polymer networks. Most importantly, this reaction consumes less energy by taking advantage of the enthalpy of the chemical reaction rather than the external energy.[35] Figure 2A shows the images acquired in a temporal sequence of a self-propagating polymerization front.[40] Robertson et al. reported DIW thermoset composites cured by the frontal polymerization reaction, as indicated in Figure 2B.[35] Their results indicated that the polymer can be cured within seconds and the printed part has a similar mechanical property to those cured by

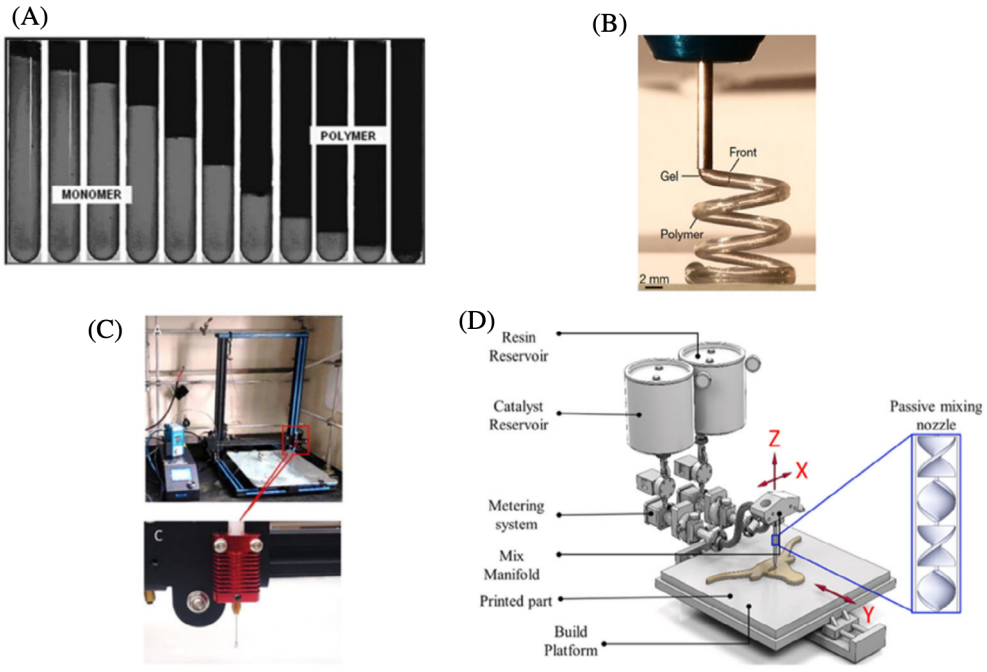

FIGURE 2 (A) The images acquired in a temporal sequence of a self-propagating polymerization front.[40] (B) DIW of DCPD solution that is extruded from the print head and then immediately cured by frontal polymerization.[35] (C) the DIW printer for the DCPD printing.[41] (D) the schematic diagram of the REAM setup[42]

the conventional methods. Wang et al. reported DIW thermosets cured by frontal thermal polymerization and investigated how the printing parameters such as nozzle pressure and operating temperature affect the thermal conductivity and surface morphology of as-printed products. Figure 2C indicates the DIW printer for their project. They concluded that there is no evident pattern observed when the extrusion pressure is higher than 75 bar and the optimal curing temperature is 75°C.[41] Uitz et al. introduced a reactive extrusion AM (REAM) process which is based on the frontal polymerization to print isotropic thermosetting parts. The thermoset resin and the curing agent were collected by separated reservoirs and mixed before DIW printing, as shown in Figure 2D.[42] The thermosets were deposited and cured by frontal polymerization reaction without any external energy. They also concluded that the tensile modulus and ultimate strength are isotropic while the break elongation and toughness are dependent on the printing orientation.

2.2 | Electromagnetic heating based in-situ curing and DIW of thermosets

Electromagnetic thermal curing is the most common curing method for thermosets. Based on the energy resource, it is typically divided into six types, including radiation thermal curing (microwave, infrared, and laser), induction thermal, ultrasonic thermal, and photothermal heat curing.[32,43] Most of these methods can conduct in-situ curing functions except induction thermal and ultrasonic heating methods. Induction thermal curing is a process that the eddy currents are generated when the electrically conductive material is exposed under a periodic alternating magnetic field.[44] The polymer would be heated because of the resistance loss of the eddy currents. According to the working principle, induction thermal curing is only suitable for thermoplastic polymer printing instead of thermosetting polymer. Orlando et al developed a fused deposition modeling (FDM)-based printer that is heated by an induction system for printing ABS polymers.[45] The principle of ultrasonic heat curing is that the heat generated by mechanical vibration will be converted by the frictional and viscoelastic effects.[46] However, there are some limitations for the fiber-reinforced composites cured by ultrasonic heating due to the serious fiber disruption.[18] Although a few studies are reporting the selective laser sintering (SHS) of thermosetting composite, the materials were mostly printed by DIW and then cured for hours by infrared laser.[11,47] Therefore, the truly efficient in-situ curing methods for thermosetting polymers are limited to (1) microwave thermal, (2) photothermal, and (3) laser thermal curing methods.

2.2.1 | Microwave heating based in-situ curing and DIW of thermosets

Microwave radiation is medium energy radiation whose frequency ranges from 300 MHz to approximately 300 GHz and the wavelength ranging from 1 to 10^3 mm.[1] Microwave thermal curing works based on the that the dielectric groups of polymers can convert the radiation energy into molecular vibrations and generate the micro-level heating via the diploe moment under the interaction with the electromagnetic field, as shown in Figure 3A.[1,20] It is also considered the most efficient volumetric thermal curing method as its very high penetration depth.[49] Odom et al. demonstrated the feasibility of applying the scanning microwave to cure additive manufacturing thermoset by a novel deposition-and-scan experiment. MWCNTs-loaded epoxy was deposited on the substrate at a constant rate of 0.16 cm/s and being exposed to microwave radiation of 1250 W. The schematic diagram of the curing process is illustrated in Figure 3B. Their results showed that the final curing temperature can reach 125°C very quickly.[20] Li et al. presented a new 3D printing method with temperature control by incorporating the prediction model and step-proportional-integral-derivative control technology. The results indicated that the microwave could achieve instantaneous and volumetric heating for the continuous carbon fiber-reinforced thermosets and the printing speed increased with the microwave power, as shown in Figure 3C. Moreover, this microwave curing method can reduce the temperature deviation to obtain a consistent tensile strength up to 358 MPa.[48]

2.2.2 | Photothermal heating based in-situ curing and DIW of thermosets

The addition of photothermal agents into thermosetting ink is another way to achieve electromagnetic thermal-induced in-situ curing for thermosets. These nanofillers can convert other energy such as photonic or electromagnetic energy into heat to initiate the curing process.[18] Photothermal curing is the most popular one and it is a process that composite ink is cured by plasmonic heating via the photothermal effect of metal nanoparticles, carbon-based nanomaterials, and metallic carbon nanotube.[50–53] Table 1 shows the photothermal conversion efficiency of the nanomaterials which can be applied for curing thermosets. From the data in Table 2, the highest conversion efficiency of carbon-based material is only around 67%. This efficiency was achieved at 0.2 W/cm^2 with a concentration of carbon-based material as 1 g/L, which is much higher than that of the Au

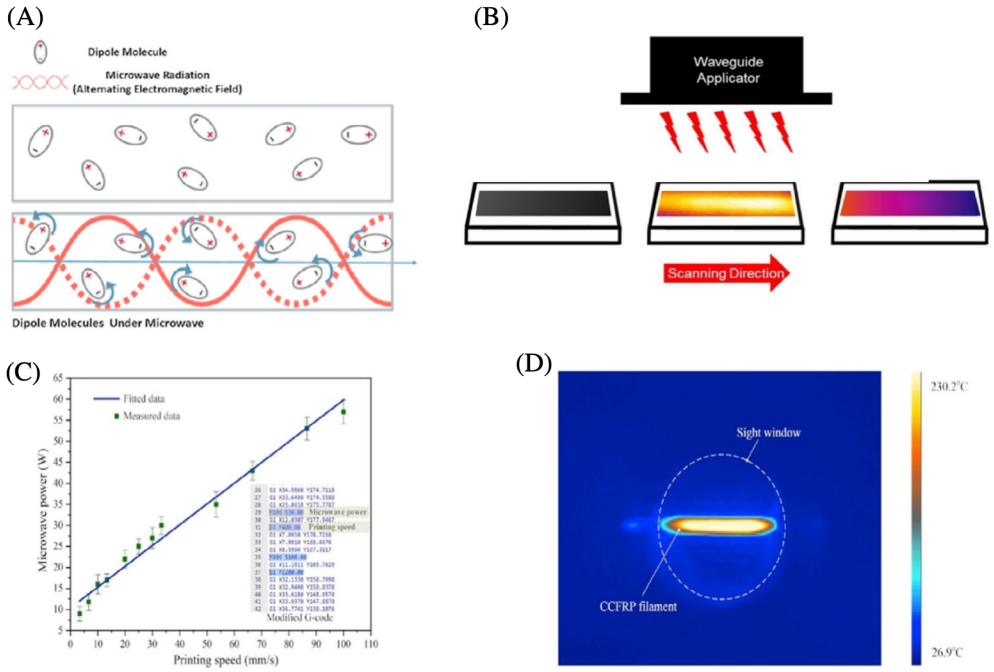

FIGURE 3 (A) Schematic illustration of the material with dipole molecules under radiation in an alternating electromagnetic field,[1] (B) schematic diagram of scanning microwave curing process,[20] (C) relationship between microwave power and printing speed.[48] (D) Colormap of temperature distribution under microwave curing

TABLE 1 The photothermal conversion efficiency of materials used in thermoset curing

Materials	Size of materials	Optical resource wavelength (nm)	Photothermal conversion efficiency (%)	Reference
Gold nanoparticle	4.98 ± 0.59 to 50.09 ± 2.34 nm	532	~65–80.3	[54]
Graphene	150 to 3000 nm (60% sample with a thickness of 1 atomic layer)	808, 980	~ 67 ~ 63	[55]
Metallic carbon nanotube	OD = 808 nm	808	~ 76	[56]
Graphene oxide	300–700 nm (60% sample with a thickness of 1 atomic layer)	808, 980	~ 58 ~ 35	[55]
Hollow Au–Ag alloy nano urchins	Sub-100 nm	808	80.4	[57]
Au nanorod	Length: 54.20 ± 2.85 nm Width: 16.37 ± 1.25 nm	750	90.6	[58]
Au@Pt nanorod	Length: 60.07 ± 4.17 nm Width: 21.97 ± 1.40 nm	810	94.8	[58]

nanomaterials. Figure 2A shows the estimated temperature versus time for conventional (filled triangles) and photothermal (open circles) curing of epoxy with Au nanoparticles.[52] Photothermal heating provided a faster temperature increase than conventional heating when the heat is applied at the shaded region. The gold nanoparticles or gold-based nanocomposites can achieve a photothermal conversion efficiency of around 94%. The suspension solution can be heated to around 65°C at a very short time, as shown in Figure 4B. However, the synthesis process of gold nanomaterials is very complex, and the price of gold is very expensive up to $65/g.[63] Although a large amount of literature reported that they can reach very high temperature and reach high conversion efficiency, the radiation time is still very long even at a high irradiation power (2 W/cm^2), which consumes too much energy.[55–57,64] Therefore, even the photothermal curing ink for DIW can be in-situ cured, it is not a cost-effective way for the curing of thermosetting polymers.

2.2.3 | Laser heating based in-situ curing and DIW of thermosets

Laser heating based in-situ curing is based on the conversion of the electromagnetic energy into heat through the

TABLE 2 Energy consumption or power input for in-situ curing methods of thermosets

In-situ curing method	Energy consumed or power input	References
Frontal polymerization	Around 6 J/cm^3	[35]
Electromagnetic heating	200–600 W at 2.45 GHz frequency (Microwave) Around 0.2 W/cm^2 (Photothermal) 18 W (Lasering heating for silicone elastomers)	[1,56,59]
Resistance thermal	1.53 Wh/cm^3	[60]
Electron beam radiation	0.22 Wh/cm^3	[37,61]
Photochemical	8 W/cm^2	[62]

molecular resonance vibration.[65,66] A CO_2 laser generator is usually applied during the curing process. Porter et al. customized an extruder and DIW printer for thermal curable viscous silicone elastomers, as shown in Figure 5A.[47] The relationship between the mechanical properties and the curing parameters such as layer thickness, laser power, laser raster spacing, print speed, and laser spot area was investigated. Their results showed that layer thickness is the most important factor in stiffness (0.73%/%). Parupelli et al. compared the performance of the DIW thermosets cured by oven and laser curing.[59] Figure 5B is the multi-axis robot printer equipped with the extrusion system, laser curing system, and jetting system. The thermosets could be cured within 1 min while it took more than 2 h in the furnace. The optimal curing parameters were obtained at a 4-pass laser at a power of 18 W. The mechanical properties of the as-printed part are comparable to those of the bulk material. Zhu et al. studied the laser-based DIW thermosets with real-time FTIR monitoring, as indicated in Figure 5C.[67] They claimed that the laser can improve the scalability of the DIW process, and the diameter of the deposition filament can reach up to 4 mm.

2.3 | Resistance thermal in-situ curing and DIW of thermosets

Another route to in-situ cure thermoset is to integrate the electrothermal material like carbon fiber or graphene which can convert the electric energy into heat via joule heating of the polymer composites.[68] Xian et al. incorporated the graphene material into the polymer matrix to take advantage of the joule heating to achieve in-situ thermal curing for thermoset polymer. As shown in Figure 5A, the results indicated that the critical loading of graphene nanoplates (GNP) is 8.5 wt% and the networks of GNP in the thermoset matrix can be used as a nano heater when there is electric current passed through it. It was also demonstrated that this curing method provides other benefits such as faster heating speed, more uniform curing, and higher energy efficiency compared with the conventional oven curing process.[36] Mas et al. also presented in-situ curing thermosets through joule heating. The nanocarbon materials (CNTs and graphene) were dispersed into the epoxy resin and cured by controlling the electric power. It is believed that this method can be applied to the composite manufacturing.[69] Shi et al. proposed a novel electrothermal-triggered flooded curing method for thermosets.[60] After DIW printing of a CNTs porous structure, the structure was dipped into liquid epoxy resin, as shown in Figure 5B. By changing the current through the CNTs, the polymer would be infiltrated and cured in a short time. They also demonstrated that this method could remove the residual bubble of the polymer by controlling the viscosity of the polymer. Shi et al. used the robot arm to print and in-situ cure continuous carbon fiber

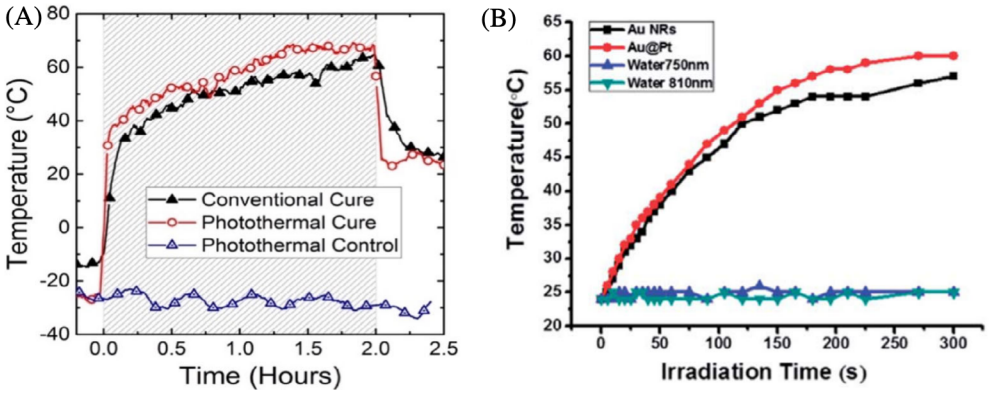

FIGURE 4 (A) The temperature change with time for different curing methods.[52] (B) the temperature change with the irradiation time for the gold nanocomposite suspension solution[58]

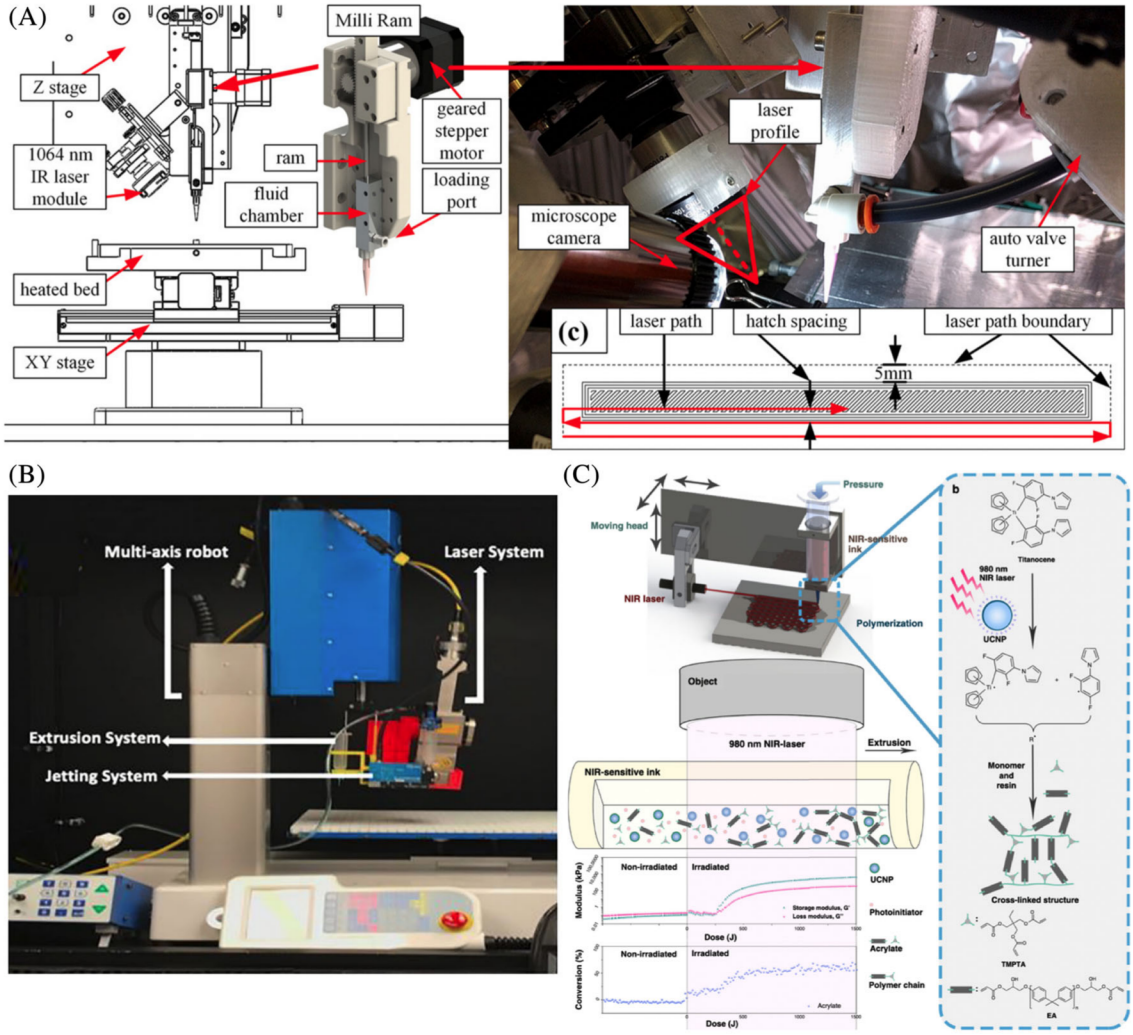

FIGURE 5 (A) Laser in-situ curing setup for DIW of thermosets.[47] (B) The multi-axis robot printer equipping with the extrusion system, laser curing system, and jetting system.[59] (C) Schematic illustration of laser-DIW and in-situ FTIR photorheology monitoring[67]

thermosetting composites.[38] The printed part has high mechanical strength (810 MPa) and modulus (108 GPa) (Figure 6).

2.4 | EB irradiation based in-situ curing and DIW thermosets

Irradiation curing is a process that the radiation-sensitive thermosets are ionized under high-energy radiation which includes γ-ray, UV, EB, and X-ray.[39] The ionic or free radical molecular from the deposition of the radiation-sensitive polymer is generated to start the curing process, which is quite different from the thermal curing process where an initiator or catalyst must be added to the polymer system to initiate the curing reaction. The γ-ray and X-ray radiation curing have been applied in the industry since the 70s.[1,70] And the two radiation curing methods usually are used to manufacture high thickness parts with a thickness of more than 300 mm due to their ultra-energy which can be greater than 100 keV.[71] The radiation frequency has an order of 10^7 GHz, and the wavelength is less than 10^{-5} mm.[1] The curing equipment system typically needs a huge power supply and a complex cooling system. As a result, there has been no literature reported yet about in-situ cured DIW thermoset by γ-ray or X-ray. Although UV curing is theoretically also an irradiation curing method, the radicals are induced by the photos. In this review, the UV curing method will be listed alone as the new category as a photochemistry-based curing method.

EB curing method is one of the irradiation curing methods that the electron beam is applied on the radiation-sensitive polymer surface and transfers adequate energy to decompose the polymer, which generates ionic or free radical to initiate the curing reaction.[39] EB is very popular in rapid manufacturing because of its high curing rate and cost-saving features.[37] Various

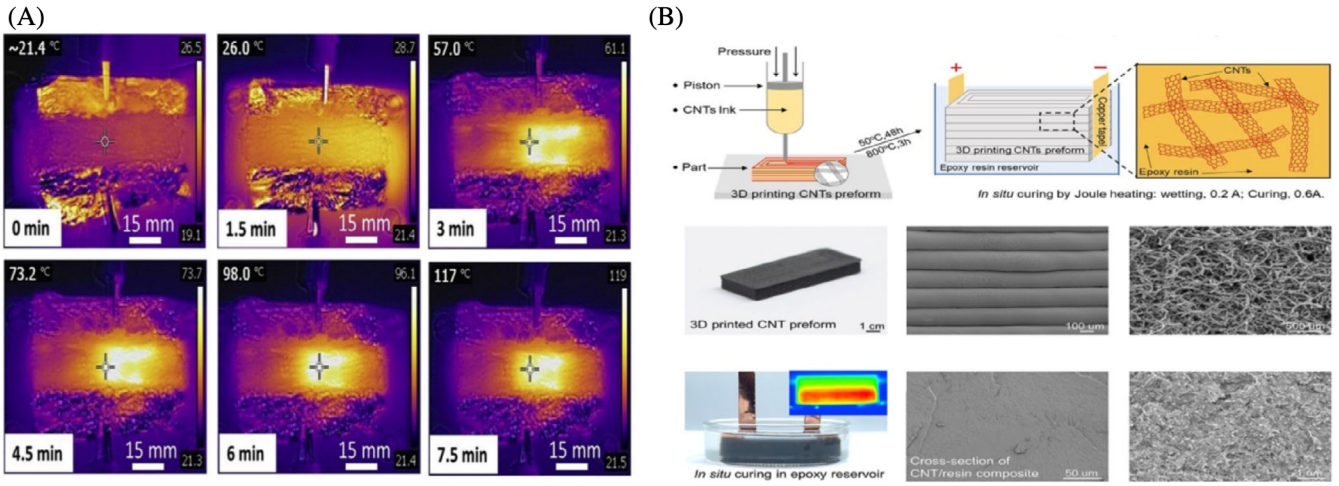

FIGURE 6 (A) Thermal images showing the temperature variation of the GNP/epoxy composite with time during the curing process.[36] (B) the DIW and electrothermal-triggered flooded curing process for thermosets[60]

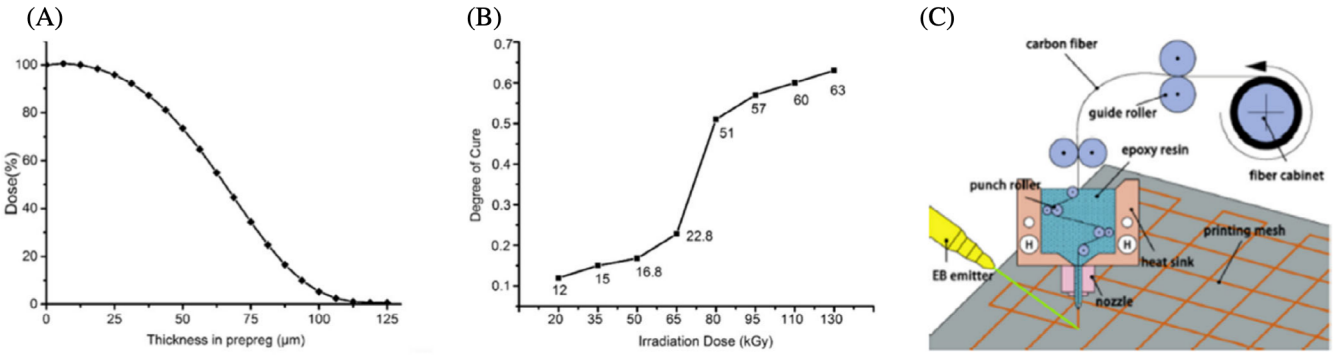

FIGURE 7 (A) The penetration thickness in prepregs under the irradiation of 125 keV.[72] (B) the relationship between the curing degree of composites and the irradiation power.[72] (C) the schematic setup of a low-energy EB cured printing process for fabricating a conductive continuous carbon fiber mesh on the surface of a wind-turbine blade[37]

types of thermosetting polymers have been proven their EB curable capability, which includes acrylics, urethane acrylates, bismaleimides, and epoxy resins. Most of those thermosets are cured through the free radical reaction except the epoxy resin. The irradiation power of the EB is proportional to the thickness of the materials. Due to the attenuation of the irradiation among the thickness, the curing degree of the polymer composites will be affected significantly. However, high power emitter can be applied to improve the curing degree or cure the whole thickness. Figure 7A shows the penetration thickness in prepregs under the irradiation of 125 keV and Figure 7B provides the relationship between the curing degree of composites and the irradiation power.[72] The results show that the curing degree increased slowly when the irradiation is below $5*10^6$ rd. There is a significant increase of curing degree between the $5*10^6$ rd and $9*10^6$ rd and it is no obvious increase after reaching $9*10^6$ rd. Wang et al. proposed a rapid curing process through low-energy EB radiation to DIW the continuous carbon fiber-reinforced thermosets as the protection system for wind-turbine blades as shown in Figure 7C.[37] They DIW the continuous carbon fiber by modifying the FFF technology in which the thermosets are printed, and in-situ cured by the low-energy EB radiation. The thermoset composites were fabricated by DIW and cured instantaneously with a high carbon fiber content (around 58 wt.%) at room temperature at a high speed. The artificial lightning strike tests indicated that the printed thermoset-carbon fiber composite protector remained a 90.1% residual strength after 100 kA current damage.[37]

2.5 | Photochemical in-situ curing and DIW of thermosets

UV curing is another in-situ curing process that UV light is applied to initiate a photochemical reaction to covert monomers into polymer networks.[16,23] There are several

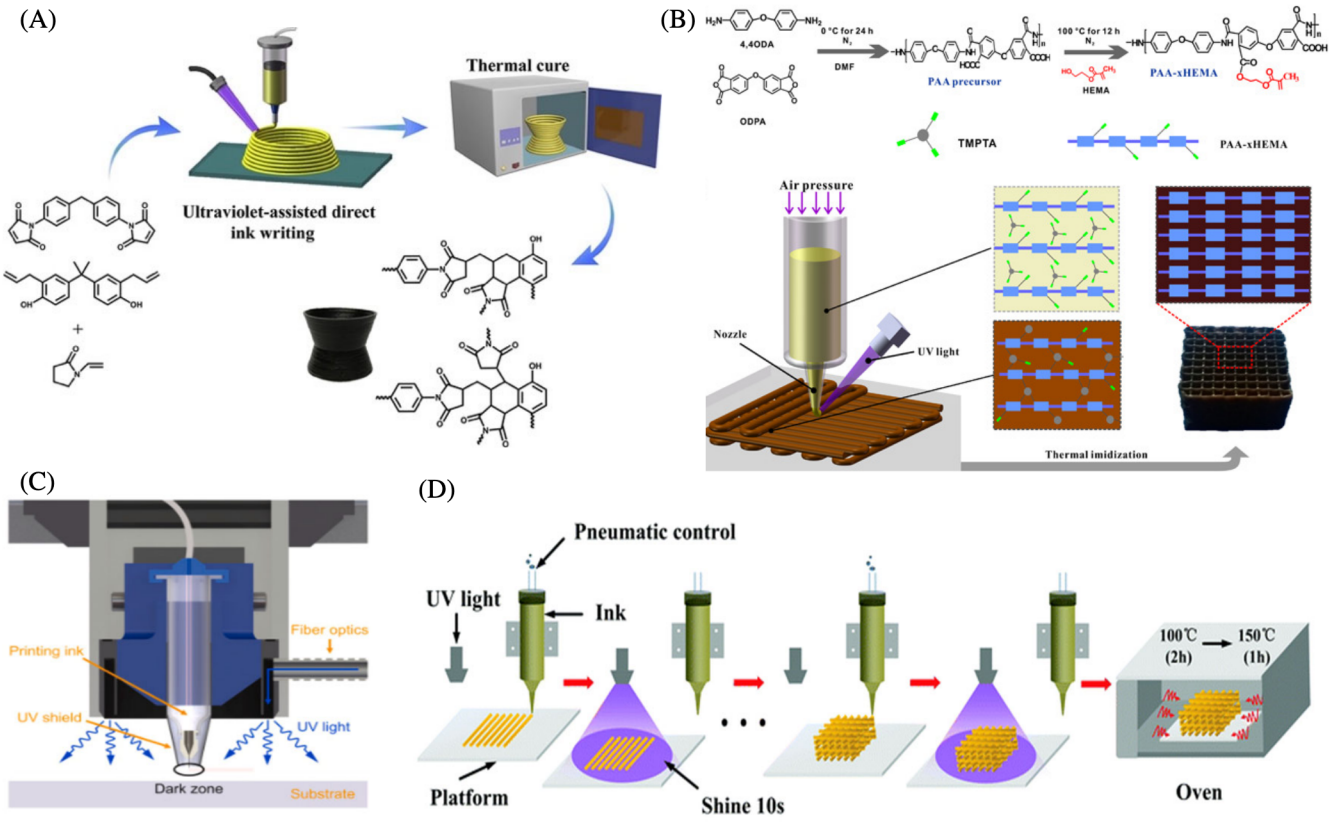

FIGURE 8 (A) An illustrative scheme of UV-assisted DIW process for the hybrid ink followed by thermal curing.[73] (B) An illustrative scheme of UV-DIW process for the hybrid ink containing polyimide.[74] (C) A schematic diagram of the modified printer with dual curing process.[75] (D) a schematic illustration of UV-assisted 3D printing of epoxy composites[76]

advantages of UV curing such as low cost, high-energy efficiency, and environment friendly. The drawback of UV curing is that it has very limited penetration depth and can only cure transparent printed parts. UV curing is usually applied to assist DIW of thermosets and a two-stage curing process is usually needed. In the UV-assisted DIW (UV-DIW) thermoset process, as shown in Figure 8A, the hybrid ink containing photocurable resin and thermally curable epoxy resin was first cured by UV to retain its geometry, and second-step curing is followed such as thermal cure in an oven to obtain the final product.[73,74,77,78] Although some literature reported one-step curing by UV, the penetration thickness of UV is rather limited so that only small-scale products can be fabricated by the UV curing method.[50,77] Guo et al. proposed a novel polyimides ink and printed by the UV-DIW method to solve the shrinkage issue of printed polyimides.[74] Figure 8B indicates the UV-DIW process for hybrid ink. The DIW polyimide was cured by a fixed UV light and then treated with an elevated temperature (up to 300°C) to initiate the thermal imidization.

Tu et al. created a UV-thermal during the curing process for vinyl ester (VE) resin printing.[75] The first stage UV curing would provide a structural geometry followed by the second stage thermal curing to allow the thermosetting monomer to cross-link. Their modified DIW printer is illustrated in Figure 8C. The printed thermosets demonstrated outstanding properties, such as Young's modulus of 3.7 GPa and the tensile strength of 80 MPa, which are higher than those of the molded neat VE resin. Chen also proved a similar two-stage curing process for epoxy in Figure 8D.[76] They introduced the epoxy oligomer into the printing ink and the epoxy oligomer formed the interpenetrating polymer networks and therefore achieved excellent shape memory properties.

2.6 | Comparison of in-situ curing methods of thermosets

There are five categories of in-situ curing methods including frontal polymerization, electromagnetic heating, electron beam irradiation, and photochemical curing for thermosets. Among these methods, frontal polymerization in-situ curing is the only method that an external energy source is not required during the curing

process except for the initiation process at the beginning of the process because of its self-propagation features. However, the initiator system is very complex in some cases and the price of the highly efficient initiator is expensive, for example, the price of *bis*[4-(tert-butyl) phenyl] iodonium Tetra (nonafluoro-tert-butoxy) aluminate is more than $200/g. The printing speed of frontal polymerization is decided by many factors such as initiator system, initiator concentration, polymer, and inhibitors.[35] The electromagnetic heating in-situ curing methods are the most widely used ones with different energy resources. There are many challenges to this method. Firstly, microwave heating may cause uneven curing because of the nonuniform power distribution within the microwave cavities and further introduce the hot spots and the wavelength of the microwave affects the penetration depth.[43] For composite material curing, especially the fiber-reinforced composites, reinforcing fiber shielding may also cause uneven curing. Secondly, photothermal heating is considered as an energy efficiency in-situ curing method since the only input energy resource is the optical light.[52] But the heat conversion efficiency of carbon-based materials (around 67%) is still lower than the gold-based material (up to around 95%). Moreover, the curing time is much longer than the conventional curing method and the light wavelength must be set at a specific value to achieve an optimal energy conversion. Finally, laser heating can cure the polymer within 1 min and the laser source is limited to the NIR-laser.[79]

Resistance thermal in-situ curing provides another energy efficiency method for in-situ curing of thermosets and shows the feasibility for scalable production for thermosets.[60] However, this method can be only used for carbon material thermosetting polymer composite other than the pure thermosets which limit its application. Electron beam irradiation holds a very high curing speed at the ambient temperature and ease of material handling. On other hand, the high-energy EB equipment is very hard to incorporate into the 3D printing system due to the complex system. The shield system made of special materials is required.[80] UV radiation curing is another popular in-situ curing method due to its economic, cost-saving features. But the low penetration depth significantly restricts its application and UV cannot cure the carbon fiber-reinforced thermosets because of the strong absorbance of UV in the carbon fiber.[81] Normally, UV is applied in the open mold condition for transparent materials. All products manufactured by the in-situ curing methods show comparable mechanical properties with the conventional cured ones. Table 2 gives the energy consumption or energy input for in-situ curing methods of thermosets.

3 | IN-SITU CURING MONITORING AND CURE KINETICS MEASUREMENT FOR THERMOSETS

In-situ curing monitoring is a direct method to observe the curing condition of thermosets during the manufacturing process since curing conditions are extremely crucial for product performance.[82] A better understanding of the thermoset curing features and the whole cure cycle would improve the product quality and help eliminate "trial-and-error" efforts in case of under-curing or premature demolding. The information on the curing process would be collected and analyzed in real-time by in-situ core monitoring. Therefore, characterization of the curing process for thermosets would assist to optimize the curing parameters for better control and prediction on the curing cycles of thermosets. The critical processing parameters such as the nozzle time and nozzle temperature for complete curing within a reduced cycle time could be solved. An appropriate curing temperature can also help avoid premature vitrification and over-high temperature that may cause some undesirable side reactions or degradation.[83]

Typically, dynamic mechanical analysis (DMA) and differential scanning calorimetry (DSC) cannot be applied directly for in-situ curing monitoring since these two measurements can only be operated under a specific condition. DSC is used to determine the exothermic heat caused by the curing process of thermosets and DMA can monitor the change of the dynamic mechanical property change during the curing process. These measurements could offer valuable information such as curing heat, glass transition temperature (T_g), initiation of the curing process, maximum curing speed, the termination of the curing process, and more importantly the curing degree of the polymer.[84] Figure 9A shows the isothermal DSC curve change with time of pure PDMS at different temperatures.[82] The curing rate increases with increasing the reaction temperature. In some cases, DSC is measured first as the baseline. Results from other characterization methods are compared with the baseline to further confirm the curing condition. Raman spectroscopy is used to monitor the rotational and vibrational transitions within the molecules and detect the composition changes of the materials during the curing process. Each chemical bond has its unique rotational and vibrational information and peaks among the spectrum corresponding to the specific chemical bond can be identified.[88]. Figure 9B presents the Raman spectra of fiber-reinforced polymers (FRPs) with time during the curing process at 80°C.[84] The characteristic peak of the epoxide group at 1255 cm^{-1} red-shifted within 120 min to illustrate the curing reaction process. The relative intensity of the peak

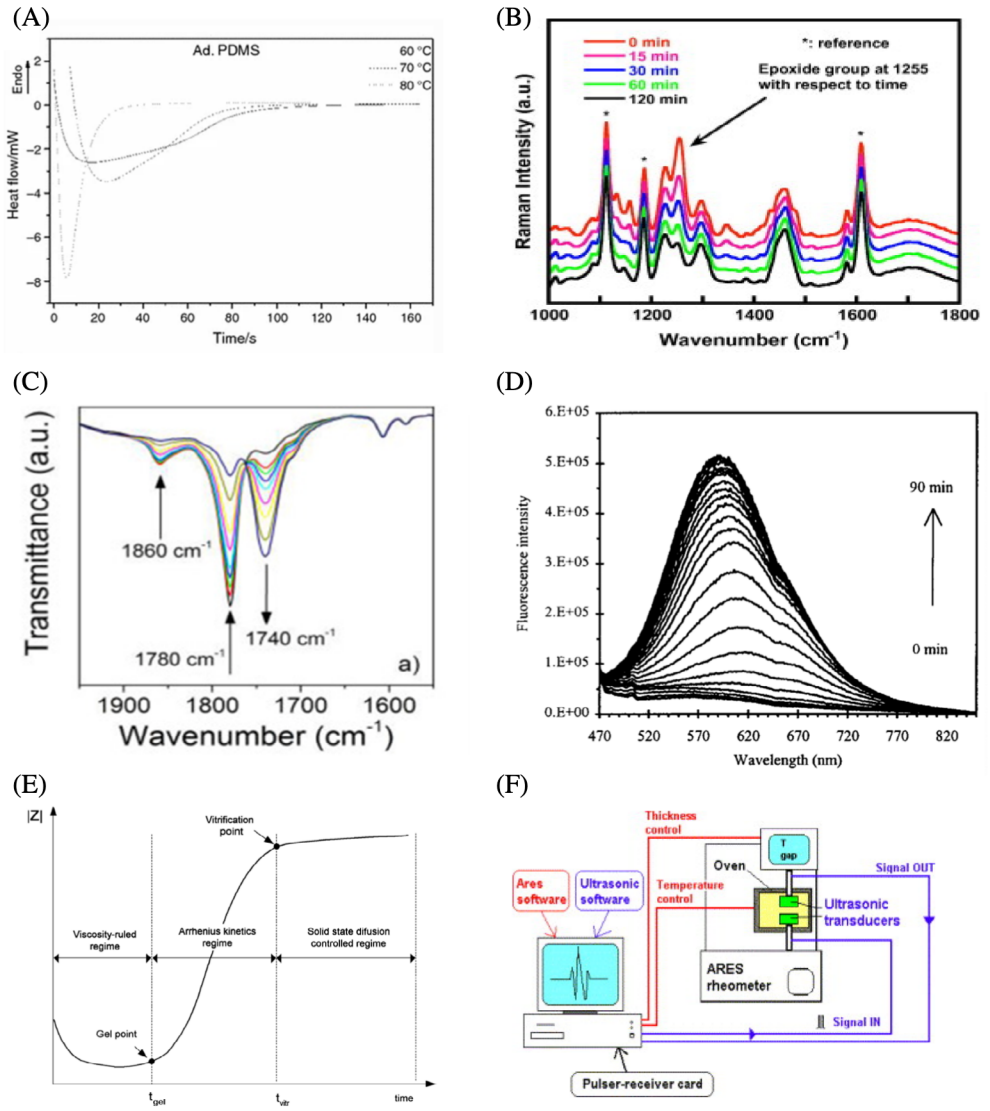

FIGURE 9 (A) The isothermal DSC curves with the time change of pure PDMS.[82] (B) the Raman spectra variation of fiber-reinforced polymers (FRPs) with time during the curing process at 80°C.[84] (C) The FT-IR spectra evolution with curing time for thermosets.[85] (D) the fluorescence spectra of epoxy resin during curing at 120°C.[86] (E) The curing stages of the dielectric analysis of polymers.[87] (F) the schematic diagram of the ultrasonic curing monitoring system.[87]

is proportional to the concentration of the composition in the sample. Other researchers also used the Raman spectra to monitor the composition of the thermosets during the curing process.[89] Optical fiber sensors can also in-situ monitor the curing process such as Fourier transform infrared spectroscopy (FT-IR), UV spectroscopy, and NIR spectroscopy. The most popular one is the FT-IR which can also record the curing state-changing by monitoring the specific peaks in the spectra, as shown in Figure 9C which is the FT-IR spectra of epoxy resin with time.[85] The curing reaction extent can be determined by observing the appearance or disappearance of specific FT-IR peaks. The peaks in 1860 and 1780 cm^{-1} decreased with time because of the depletion of the stretching of C═O bonds from the hardener while the peak at 1740 cm^{-1} increased with time due to the formation of the ester groups during the curing process. Fluorescence spectroscopy is also widely used for in-situ cure monitoring due to its high sensitivity and nondestructive features.[86,90] This measurement is based on the interaction between the fluorophore molecules and their surroundings. The most significant feature is that there is a fluorescence wavelength shift for some fluorescence dyes because of the refractive index of thermosets increasing and their dipolar mobility decreasing.[90] Figure 9D presents a fluorescence spectrum of epoxy resin during the curing process.[86] As the curing process proceeded, the fluorescence intensity increased, as the arrow indicates.

Broadband dielectric spectroscopy (BDS), alternatively named dielectric analysis (DEA) is also an important measuring method for in-situ cure monitoring.[91] Figure 9E shows the curing stages observed by BDS.[92,93] The dielectric response is proportional to the ionic conductivity of the impurity and chemicals applied in the curing process. At the first stage, there was a decreasing trend of the dielectric response due to the higher mobility of the impurity. At the second stage, the curing reaction started improving the polymer viscosity

increasing the impedance which follows the Arrhenius kinetics rule. Finally, the solid-state diffusion governed the region that a longer time is needed to finish the curing process. However, the BDS measurement is sometimes non-isothermal, and the preferred frequency range is not broad as enough as expected.[94] Ultrasonic dynamic analysis (UDMA) as a high-frequency extension of the DMA approach has received significant attention.[95,96] The velocity and attenuation of the ultrasonic waves are measured in real-time to provide the viscoelastic information of the polymer networks to achieve cure monitoring. Figure 9F is a schematic diagram of the ultrasonic cure monitoring setup which consists of two ultrasonic probes.[87] However, this kind of setup is expensive and very complex. There are also some other technologies available for curing monitoring such as piezoelectric sensors and microdielectrometry.[90,97,98]

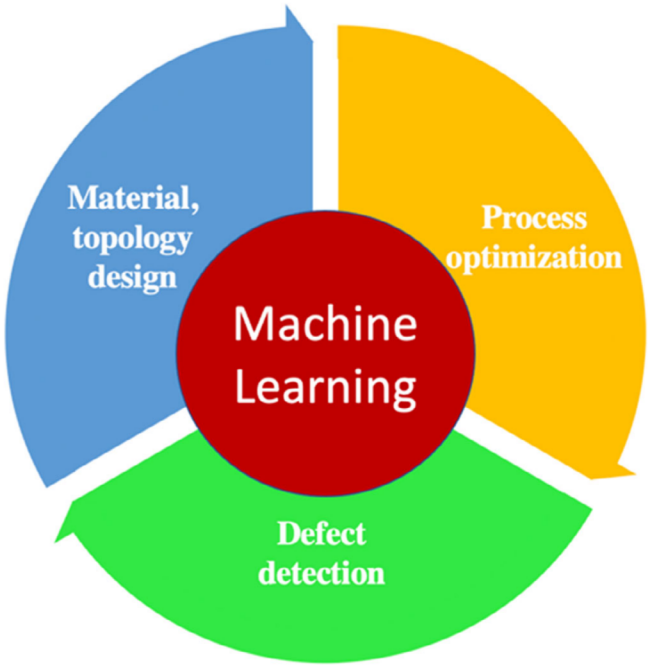

FIGURE 10 The application of ML in the stages of DIW of thermosets

4 | PROCESS CONTROL AND MONITORING OPTIMIZATION BY STATE-OF-ART MACHINE LEARNING FOR DIW THERMOSETS

ML has attracted attention for AM since these technologies can dramatically eliminate inconsistency problems during and after the printing/curing process. With the significantly increasing demand for the manufacturing of products with complex geometry, machine learning has been implemented to detect flaws of printed parts and optimize their printing parameters.[24] Based on the ML algorithms applied in AM, supervised learning, reinforcement learning, and unsupervised learning are three main methods that can help obtain the desired results by data training or achieve the optimal products through minimizing human supervision while maintaining satisfactory performance. Except for the simple regression and support vector machine which are the most popular ones, neural networks have also gained considerable attention from researchers because of their ability to build complex networks in the model and wide application in image recognition, self-driving, search engine, and language processing. However, enough inputs with more detailed information of the predicted condition are required by neural networks to improve the accuracy and usability of the model. This would bring another challenge that is extracting the inputs in a rapid and sample way. For instance, for the prediction of the DIW thermosets performance based on the part geometry, neutral networks need a rapid and automatic data acquisition of the product images by computer vision. The application of ML for the DIW thermosets is classified into three stages: material and topology design, printing parameter optimization, and performance and quality control, as illustrated in Figure 10. This part will follow these three stages to give a brief review of ML in DIW and curing control for thermosets.

4.1 | Material and topology design for thermoset

Composites with excellent performance have been over many decades. These high-performance materials were designed and explored manually with thousands of possible combinations, which is time-consuming and challenging.[99] ML can reduce the burden of the calculation and experiment and accelerate the discovery processing of novel materials with desired properties. Yan et al proposed a couple of methodologies to solve the small dataset of the strain and stress results, inadequate structure information of multiscale and intractable feature of fingerprinting based on the ML to assist the discovery of novel thermoset shape memory polymers (TSMPs), as present in Figure 11A.[100] By applying the dual convolution model, linear notation Big SMILES for fingerprinting, and a mixed 1D and 2D input model, 14 novel TSMPs with better recovery stress were discovered through 4459 samples. Also, a molecular dynamics model was conducted to confirm one of the 14 new thermosets. Gu et al studied the feasibility and capacity of ML to

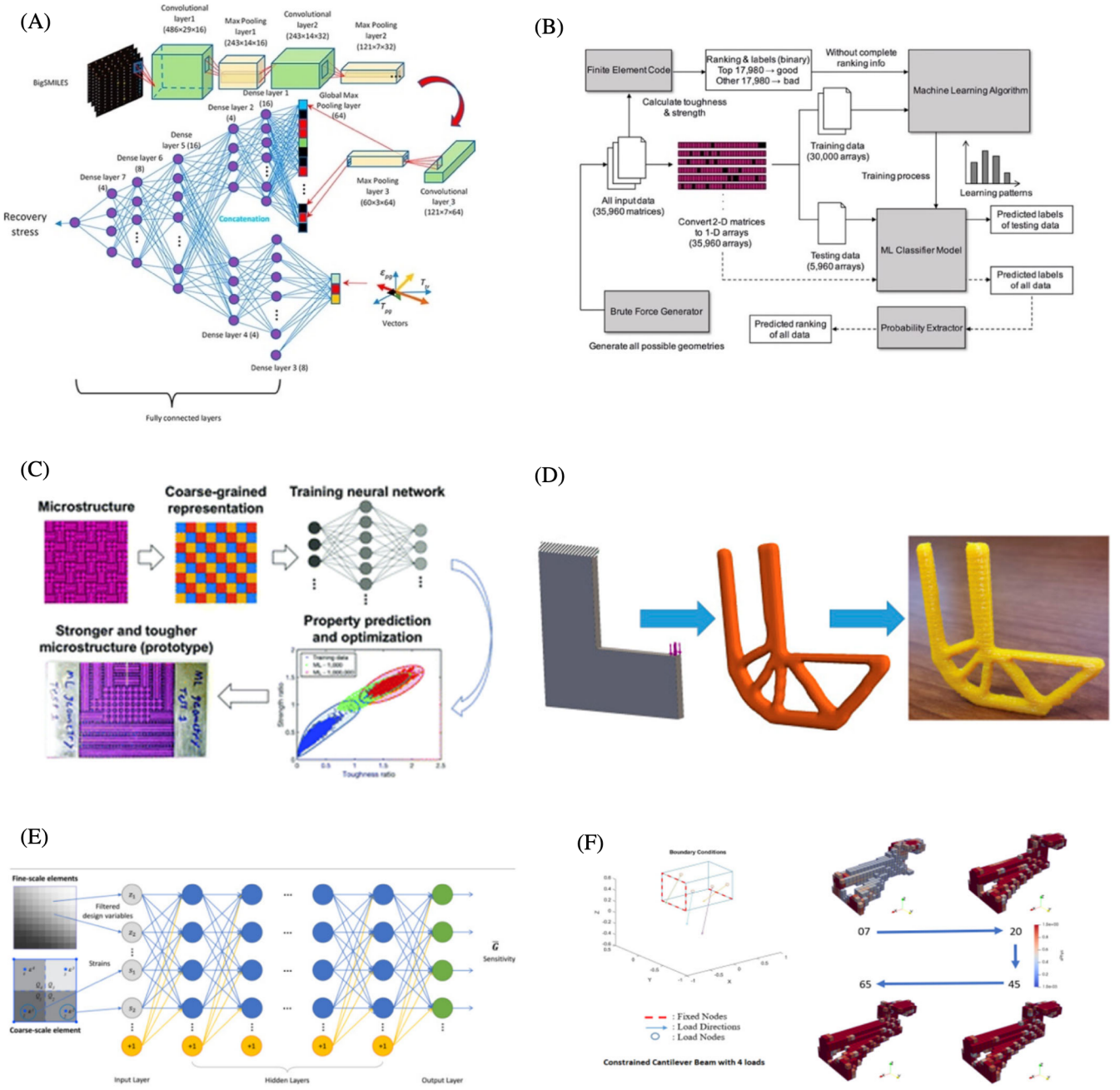

FIGURE 11 (A) The methodology of the discovery of TSMPs by ML.[100] (B) The overall flowchart describes the ML by applying a linear model for an 8 by 8 system.[101] (C) The hierarchical design construction and the application of ML.[102] (D) The application of TO design in additive manufacturing.[103] (E) The architecture of deep neural network for topology optimization.[104] (F) The iterative process of the SIMP TO optimization[105]

predict the mechanical property of composites.[101] They proposed a new design methodology called De novo composite design based on ML technology. The optimum design parameters were generated with an efficient computational cost and accuracy. Their results demonstrate the feasibility of ML application in the field of composite design and concluded that ML is a promising approach for novel multifactional and customizable composite discovery. Inspired by biomimicry, Gu et al designed a hierarchical composite to achieve excellent mechanical properties.[102] They came up with a model with a distinct region of unit cell which is shown in Figure 11C. The composite structure consists of a group of soft and stiff blocks that are constructed to get the symmetric and asymmetric mechanical behavior. A printed thermosetting part was used to evaluate the ML-assisted design. Topology design is a systematic technology that is used to design high-performance structures and improve

manufacturing efficiency with minimal and priori designs.[106–108] AM can significantly reduce the manufacturing difficulty of some parts obtained from the topology design with complicated shapes. As illustrated in Figure 11D, the structure problem was optimized by the topology design, and finally printed to get the final product.[103] There are several challenges in the topology optimization (TO) for the AM process.[109] Many iterations of a design are required by the traditional TO process, however, the ML can output the desired design fast by well-trained models through deep neural networks.[110] Chi et al. proposed a general ML-based for deterministic topology optimization.[104] The framework can improve the efficiency of large-scale design problems significantly and retain accuracy at the same time. The architecture of the neural network is shown in Figure 11E. There is an encoder network that is composed of six convolutional layers and a decoder network that has the same structure in the model. A final pixel-wise classification layer was followed. The results demonstrated that the model has a good generalization property and quick acceleration of the optimization process. Banga et al. also studied the deep learning method to accelerate TO by the convolutional neural network (CNN), as presented in Figure 11F.[105] 40% reduction of computation time and 96% improvement of structural accuracies were achieved by the well-trained network.

4.2 | Process optimization for thermosets

Conventional process optimization methods, such as the design of experiments are time-consuming and have too many combinations of parameters, which makes the

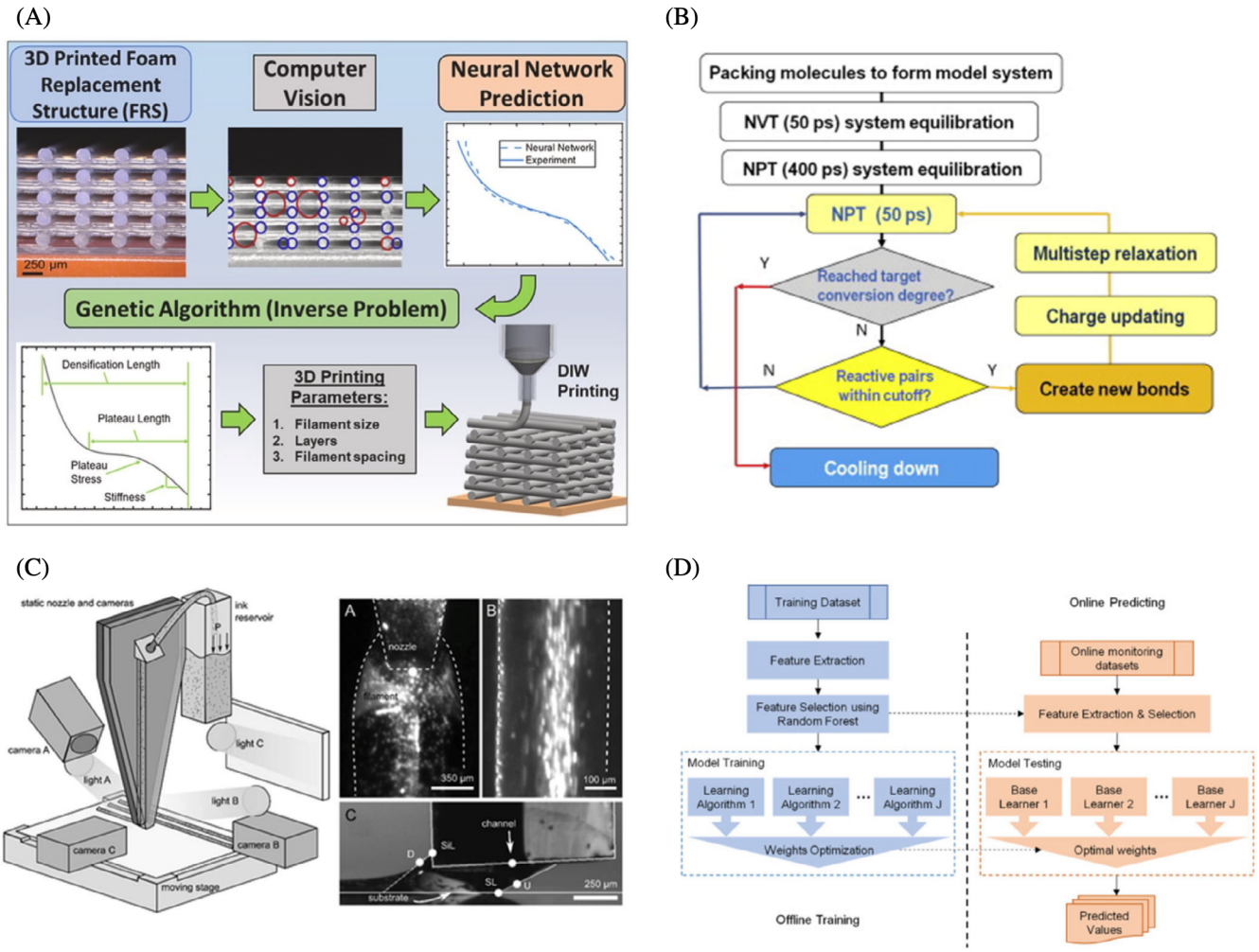

FIGURE 12 (A) The combination of computer vision, neural network, and genetic algorithm for DIW thermosetting foam materials.[116] (B) The flowchart of the curing process optimization process.[117] (C) DIW printing system with monitoring system.[118] (D) The ML prediction modeling flow chart for surface roughness[119]

optimization process computationally costly.[25,26,111] As a result, ML has also been applied to process optimization to solve those challenges.[112] This section will provide an understanding of how the ML can be used to affect the performance of the printed parts. Computer vision also has a wide application in the industry and our daily life such as self-driving, packing, and individual health monitoring.[113,114] Digital image correlation theory is to collect the data of the structure displacement changing with time to analyze and predict the printed product performance and get the optimal printing parameters.[115] Roach et al. developed a novel method to predict the mechanical properties of DIW thermosetting foam replacement materials by training neural networks from the images of the cross-section area and developing a computer vision algorithm to investigate the relationship between images and the mechanical properties, as shown in Figure 12A. They developed a genetic algorithm (GA) to generate the printing parameters for desired compression response of DIW thermosets. Besides, molecular dynamics (MD) modeling simulator was created to simulate the curing process for the thermosets.[120] The simulation consists of three stages including the pre-crosslinking, crosslinking, and annealing stage, which is described in Figure 12B. Kravchenko et al. studied the thermal strains by a multi-scale model which can separate the cure

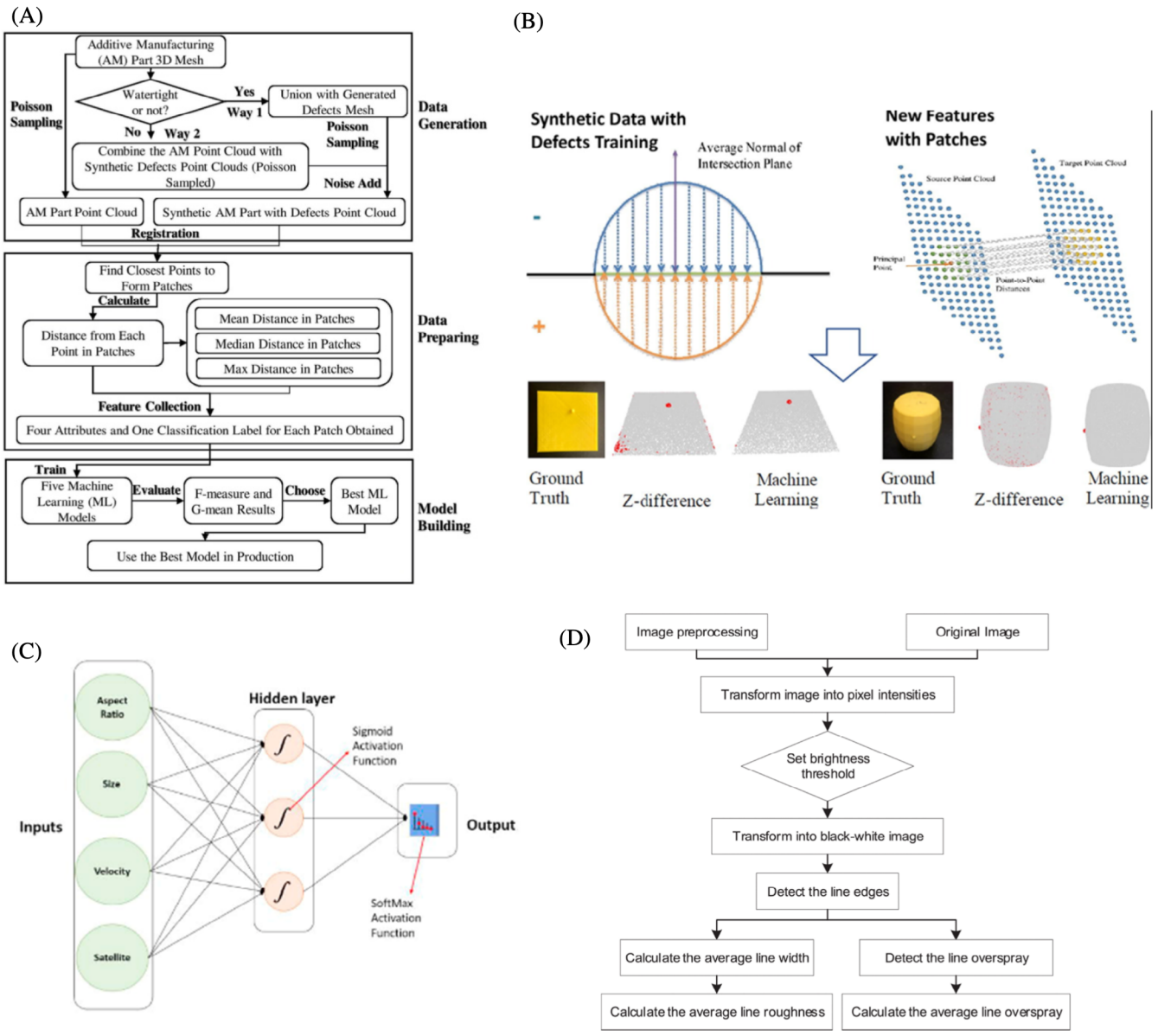

FIGURE 13 (A) The schematic three-step framework (data generation, data preparation, and model building).[125] (B) The concept "patch" application for defect detection in ML.[125] (C) The BPNN neural network for in-situ monitoring of the printing process.[127] (D) The flowchart of image processing for line edges and overspray[128]

shrinkage and thermal expansion.[117] They claimed that this model can provide the optimal curing cycles which have the minimum curing shrinkage. Friedrich et al. applied the in-situ image analysis into the DIW.[118] Figure 12C is the DIW printing system with the monitoring system and the right part showed the printing process captured by a camera. The lubrication theory was implemented to optimize the printing parameters and experiments were conducted to evaluate the accuracy of the theory and simulation. The extracted metrics such as linear regression, Gaussian smoothing, and nonlinear regression were used as the predictors to optimize the printed part with gradient structures and properties. Li et al. discussed the ML model for surface roughness prediction for additive manufacturing. The model includes offline model training and online prediction, as shown in Figure 12D. The data was collected by the sensor and trained by the ensemble ML model which combined six different algorithms. The results showed the model can predict the surface roughness of printed parts precisely.

4.3 | Defect detection for thermosets

Various defects will be generated during the AM process because of the improper printing parameters.[121,122] The defect detection is typically obtained by inspection after the printing, which is highly based on the experience of the operator.[123–125] As a result, the correction process may take a long time and be inaccurate. An ML-assisted in-situ monitoring system has been applied in defect detection effectively.[126] Li et al. proposed a new framework based on the ML model and synthetic dataset, as shown in Figure 13A.[125] The synthetic 3D defect point clouds were applied to train the model and then the real production. Instead of measuring the distance between the source and target points clouds. A novel concept named "patch" was proposed and used to capture the near-by point information in the macro-level for the ML training which is presented in Figure 13B. Ogunsanya et al. studied the backpropagation neural network model (BPNN) which is shown in Figure 13C.[127] A 90% accuracy was obtained for droplet monitoring for injecting 3D printing. Zhang et al also applied the ML for the overspray detection.[128]

5 | CONCLUSION AND FUTURE DIRECTION

DIW has been proven to be an effective way for fabricating high-performance thermosets in the automotive, aerospace, defense, wind energy, and construction industry. Rapid in-situ curing plays a crucial role in thermosets manufacturing because of its energy-saving and scalable features. Many in-curing methods have been developed for thermoset curing but only some of them are successfully applied for real-time curing of DIW thermosets. The current research progress of the in-situ curing method is reviewed, and the disadvantages of those methods are discussed. Based on the working mechanism and energy resource, in-situ curing methods are categorized into five species including frontal polymerization, electromagnetic heating, photochemistry, electron beam, and resistance heating curing. The in-situ curing motioning, characterization, and cure kinetics research methods provided an important pathway for the quality control of DIW thermoset products. Furthermore, ML technologies have been applied to optimize the printing and curing processes. The ML application in design, printing parameter optimization, and defect detection area will provide a time-efficient control and guideline to the whole DIW process.

For future manufacturing, the highly efficient power source will become the leading in-situ curing energy source. In addition, the development of sample radiation generators instead of using current cumbersome setups will significantly reduce the in-situ curing cycle. Considering the limited efficiency and relatively long curing time of photothermal curing, some novel 2D material can be added to improve the photothermal efficiency to accelerate the curing speed and temperature. The current frontal curing method needs a complex initiator system, and the pot life of the ink is limited. Therefore, one component initiator would be a significant advance. Furthermore, when UV curing is used, more two-step curing methods should be developed to overcome the limitation of UV curing, and a more effective UV-sensitive initiator needs to be developed. Most important of all, recent reports suggest that 3D printing technology is gaining a breakthrough and possibly reaching a take-off point within the next decade. The trend toward this smart manufacturing technology will become more focused on the development of more smart material inks that can be used for additive manufacturing. More computational tools such as machine learning and artificial intelligence have been applied to optimize the in-situ curing process or search for a novel material/structure design. In the future, additive manufacturing will be further combined with artificial intelligence, machine learning, and digital security to provide more efficient "make-on-demand" and "make-on-site" experiences.

ACKNOWLEDGMENTS

Authors are grateful for the funding support from National Science Foundation (CMMI-1934120, CMMI-1933679).

AUTHOR CONTRIBUTIONS

Chongjie Gao: Conceptualization (equal); formal analysis (equal); investigation (equal); writing – original draft (equal); writing – review and editing (equal). **Jingjing Qiu:** Conceptualization (equal); project administration (equal); writing – review and editing (equal). **Shiren Wang:** Conceptualization (lead); project administration (lead); supervision (lead); writing – review and editing (supporting).

DATA AVAILABILITY STATEMENT

Data openly available in a public repository that issues datasets with DOIs.

ORCID

Shiren Wang https://orcid.org/0000-0003-4516-3025

REFERENCE

[1] C. O. Mgbemena, D. Li, M. F. Lin, P. D. Liddel, K. B. Katnam, V. K. Thakur, H. Y. Nezhad, *Compos, Part A Appl. Sci. Manuf.* **2018**, *115*, 88.
[2] B. Wang, Z. Zhang, Z. Pei, J. Qiu, S. Wang, *Adv. Compos. Hybrid Mater.* **2020**, *3*, 1.
[3] H. Ku, H. Wang, N. Pattarachaiyakoop, M. Trada, *Compos, Part B* **2011**, *42*(4), 856.
[4] X. Huang, P. Jiang, T. Tanaka, *IEEE Electr. Insul. Mag.* **2011**, *27*(4), 8.
[5] A. Rahman, I. Ali, S. M. Al Zahrani, R. H. Eleithy, *Nano* **2011**, *6*(03), 185.
[6] G. D. Goh, Y. L. Yap, S. Agarwala, W. Y. Yeong, *Adv. Mater. Technol.* **2019**, *4*(1), 1800271.
[7] T. Sathishkumar, S. Satheeshkumar, J. Naveen, *J. Reinf. Plast. Compos.* **2014**, *33*(13), 1258.
[8] M. B. A. Tamez, I. Taha, *Addit. Manuf.* **2020**, *37*, 101748.
[9] M. R. Matsen, *Energy Efficient Thermoplastic Composite Manufacturing*, Boeing Research and Technology, Seattle, WA **2020**.
[10] K. Yang, J. C. Grant, P. Lamey, A. Joshi-Imre, B. R. Lund, R. A. Smaldone, W. Voit, *Adv. Funct. Mater.* **2017**, *27*(24), 1700318.
[11] C. G. Campbell, D. J. Astorga, E. Martinez, M. Celina, *MRS Commun.* **2021**, *11*, 1.
[12] M. Yakout, M. Elbestawi, presented at 6th Int. Conf. Virtual Mach. Process Technol. Montréal, May 29th–June 2nd, 2017.
[13] Y. Zhang, G. Shi, J. Qin, S. E. Lowe, S. Zhang, H. Zhao, Y. L. Zhong, *ACS Appl. Electron. Mater.* **2019**, *1*(9), 1718.
[14] G. Shi, S. E. Lowe, A. J. T. Teo, T. K. Dinh, S. H. Tan, J. Qin, Y. Zhang, Y. L. Zhong, H. Zhao, *Appl. Mater. Today* **2019**, *16*, 482.
[15] V. G. Rocha, E. Saiz, I. S. Tirichenko, E. García-Tuñón, *J. Mater. Chem. A* **2020**, *8*(31), 15646.
[16] D. Åkesson, M. Skrifvars, S. Lv, W. Shi, K. Adekunle, J. Seppälä, M. Turunen, *Prog. Org. Coat.* **2010**, *67*(3), 281.
[17] H. A. Hegab, *Manuf. Rev.* **2016**, *3*, 11.
[18] D. Abliz, Y. Duan, L. Steuernagel, L. Xie, D. Li, G. Ziegmann, *Polym. Polym. Compos.* **2013**, *21*(6), 341.
[19] S. Rezaeimalek, J. Huang, S. Bin-Shafique, *Constr. Build. Mater.* **2017**, *146*, 210.
[20] M. G. Odom, C. B. Sweeney, D. Parviz, L. P. Sill, M. A. Saed, M. J. Green, *Carbon* **2017**, *120*, 447.
[21] S. Minakuchi, *J. Compos. Mater.* **2015**, *49*(9), 1021.
[22] X. Xu, Y. Zhang, J. Jiang, H. Wang, X. Zhao, Q. Li, W. Lu, *Compos. Sci. Technol.* **2017**, *149*, 20.
[23] Y. C. Kim, S. Hong, H. Sun, M. G. Kim, K. Choi, J. Cho, H. R. Choi, J. C. Koo, H. Moon, D. Byun, K. J. Kim, J. Suhr, S. H. Kim, J. D. Nam, *Eur. Polym. J.* **2017**, *93*, 140.
[24] Z. Jin, Z. Zhang, K. Demir, G. X. Gu, *Matter* **2020**, *3*(5), 1541.
[25] F. W. Baumann, A. Sekulla, M. Hassler, B. Himpel, M. Pfeil, *Int. J. Rapid Manuf.* **2018**, *7*(4), 310.
[26] X. Qi, G. Chen, Y. Li, X. Cheng, C. Li, *Therm. Eng.* **2019**, *5*(4), 721.
[27] Z. Zhang, K. Friedrich, *Compos. Sci. Technol.* **2003**, *63*(14), 2029.
[28] H. Zhang, S. K. Moon, *ACS Appl. Mater. Interfaces* **2021**, *13*, 53323.
[29] C. Wang, X. P. Tan, S. B. Tor, C. S. Lim, *Addit. Manuf.* **2020**, *36*, 101538.
[30] L. Meng, B. McWilliams, W. Jarosinski, H. Y. Park, Y. G. Jung, J. Lee, J. Zhang, *JOM* **2020**, *72*(6), 2363.
[31] J. Morgan, M. Halton, Y. Qiao, J. G. Breslin, *J. Manuf. Syst.* **2021**, *59*, 481.
[32] D. Lei, Y. Yang, Z. Liu, S. Chen, B. Song, A. Shen, B. Yang, S. Li, Z. Yuan, Q. Qi, L. Sun, Y. Guo, H. Zuo, S. Huang, Q. Yang, X. Mo, C. He, B. Zhu, E. M. Jeffries, F. L. Qing, X. Ye, Q. Zhao, Z. You, *Mater. Horiz.* **2019**, *6*(2), 394.
[33] L. Li, Q. Lin, M. Tang, A. J. E. Duncan, C. Ke, *Chem. A Eur. J.* **2019**, *25*(46), 10768.
[34] X. Kuang, Z. Zhao, K. Chen, D. Fang, G. Kang, H. J. Qi, *Macromol. Rapid Commun.* **2018**, *39*(7), 1700809.
[35] I. D. Robertson, M. Yourdkhani, P. J. Centellas, J. E. Aw, D. G. Ivanoff, E. Goli, E. M. Lloyd, L. M. Dean, N. R. Sottos, P. H. Geubelle, J. S. Moore, S. R. White, *Nature* **2018**, *557*(7704), 223.
[36] T. Xia, D. Zeng, Z. Li, R. J. Young, C. Vallés, I. A. Kinloch, *Compos. Sci. Technol.* **2018**, *164*, 304.
[37] B. Wang, Y. Ming, Y. Zhu, X. Yao, G. Ziegmann, H. Xiao, X. Zhang, J. Zhang, Y. Duan, J. Sun, *Addit. Manuf.* **2020**, *31*, 100967.
[38] B. Shi, Y. Shang, P. Zhang, A. P. Cuadros, J. Qu, B. Sun, B. Gu, T. W. Chou, K. (. K.). Fu, *Matter* **2020**, *2*(6), 1594.
[39] J. Hay, P. O'Gara, *Proc. Inst. Mech. Eng.* **2006**, *220*(3), 187.
[40] Y. V. Kissin, A. J. Brandolini, J. L. Garlick, *J. Polym. Sci., Part A: Polym. Chem.* **2008**, *46*(16), 5315.
[41] B. Wang, K. F. Arias, Z. Zhang, Y. Liu, Z. Jiang, H. J. Sue, N. Currie-Gregg, S. Bouslog, Z. (. Z. J.). Pei, S. Wang, *Manuf. Lett.* **2019**, *21*, 1.
[42] O. Uitz, P. Koirala, M. Tehrani, C. C. Seepersad, *Addit. Manuf.* **2021**, *41*, 101919.
[43] T. Chaowasakoo, N. Sombatsompop, *Compos. Sci. Technol.* **2007**, *67*(11–12), 2282.
[44] M. Roy, P. Tran, T. Dickens, A. Schrand, *J. Compos. Sci.* **2020**, *4*(1), 1.
[45] Carter, W.G., R. Orlando, R. R. Akers, W. A. Morrison, presented at Low-cost Electromag. Heat. Technol. Polym. Extr.

Addit. Manuf. Oak Ridge National Lab.(ORNL), Oak Ridge, TN, 2016.
[46] I. F. Villegas, R. van Moorleghem, *Compos, Part A Appl. Sci. Manuf.* **2018**, *109*, 75.
[47] D. A. Porter, N. Davis, P. S. Krueger, A. L. Cohen, D. Son, *Rapid Prototyping J.* **2020**, *26*, 145.
[48] N. Li, G. Link, J. Jelonnek, *Compos. Sci. Technol.* **2020**, *187*, 107939.
[49] F. Boey, B. Yap, *Polym. Test.* **2001**, *20*(8), 837.
[50] X. Wan, L. Luo, Y. Liu, J. Leng, *Adv. Sci.* **2020**, *7*(16), 2001000.
[51] R. J. Fortenbaugh, B. J. Lear, *Nanoscale* **2017**, *9*(25), 8555.
[52] J. Dong, G. E. Firestone, J. R. Bochinski, L. I. Clarke, R. E. Gorga, *Nanotechnology* **2017**, *28*(6), 065601.
[53] A. H. Bonardi, F. Bonardi, F. Dumur, D. Gigmes, J. P. Fouassier, J. Lalevée, *Macromol. Rapid Commun.* **2019**, *40*(23), 1900495.
[54] K. Jiang, D. A. Smith, A. Pinchuk, *J. Phys. Chem. C* **2013**, *117*(51), 27073.
[55] O. A. Savchuk, J. J. Carvajal, J. Massons, M. Aguiló, F. Díaz, *Carbon* **2016**, *103*, 134.
[56] J. Song, F. Wang, X. Yang, B. Ning, M. G. Harp, S. H. Culp, S. Hu, P. Huang, L. Nie, J. Chen, X. Chen, *J. Am. Chem. Soc.* **2016**, *138*(22), 7005.
[57] Z. Liu, L. Cheng, L. Zhang, Z. Yang, Z. Liu, J. Fang, *Biomaterials* **2014**, *35*(13), 4099.
[58] J. Tang, X. Jiang, L. Wang, H. Zhang, Z. Hu, Y. Liu, X. Wu, C. Chen, *Nanoscale* **2014**, *6*(7), 3670.
[59] S. K. Parupelli, S. Desai, *Int. J. Adv. Manuf. Technol.* **2020**, *110*(1), 543.
[60] B. Shi, Y. Shang, P. Zhang, S. Liu, S. Huang, B. Sun, B. Gu, K. (. K.). Fu, *Compos. Sci. Technol.* **2020**, *200*, 108409.
[61] Z. Y. Zhang, M. J. Xu, B. Li, *J. Appl. Polym. Sci.* **2017**, *134*(24), 44959.
[62] T. Rathschlag, *Phys. Sci. Rev.* **2021**, *6*, 20200162. https://doi.org/10.1515/psr-2020-0162.
[63] A. Jain, P. C. Biswal, *Resour. Policy* **2016**, *49*, 179.
[64] P. Huang, J. Lin, W. Li, P. Rong, Z. Wang, S. Wang, X. Wang, X. Sun, M. Aronova, G. Niu, R. D. Leapman, Z. Nie, X. Chen, *Am. Ethnol.* **2013**, *125*(52), 14208.
[65] X. Wang, D. Y. Lou, *Int. J. Energy Res.* **2003**, *27*(4), 377.
[66] Z. Hong, R. Liang, *Sci. Rep.* **2017**, *7*(1), 1.
[67] J. Zhu, Q. Zhang, T. Yang, Y. Liu, R. Liu, *Nat. Commun.* **2020**, *11*(1), 1.
[68] C. Joseph, C. Viney, *Compos. Sci. Technol.* **2000**, *60*(2), 315.
[69] B. Mas, J. P. Fernández-Blázquez, J. Duval, H. Bunyan, J. J. Vilatela, *Carbon* **2013**, *63*, 523.
[70] C. Dispenza, S. Alessi, G. Spadaro, *Adv. Polym. Technol. J. Polym. Process. Inst.* **2008**, *27*(3), 163.
[71] J. Halpern, S. Holt, *Nature* **1992**, *357*(6375), 222.
[72] J. Zhang, Y. Duan, X. Zhao, B. Wang, *J. Appl. Polym. Sci.* **2017**, *134*(24), 44944.
[73] T. Wu, P. Jiang, X. Zhang, Y. Guo, Z. Ji, X. Jia, X. Wang, F. Zhou, W. Liu, *Mater. Des.* **2019**, *180*, 107947.
[74] Y. Guo, J. Xu, C. Yan, Y. Chen, X. Zhang, X. Jia, Y. Liu, X. Wang, F. Zhou, *Adv. Eng. Mater.* **2019**, *21*(5), 1801314.
[75] R. Tu, H. A. Sodano, *Addit. Manuf.* **2021**, *46*, 102180.
[76] K. Chen, X. Kuang, V. Li, G. Kang, H. J. Qi, *Soft Matter* **2018**, *14*(10), 1879.
[77] K. Chen, L. Zhang, X. Kuang, V. Li, M. Lei, G. Kang, Z. L. Wang, H. J. Qi, *Adv. Funct. Mater.* **2019**, *29*(33), 1903568.
[78] Y. Cui, J. Yang, D. Lei, J. Su, *Ind. Eng. Chem. Res.* **2020**, *59*(25), 11381.
[79] C. Schmitz, B. Strehmel, *J. Coat. Technol. Res.* **2019**, *16*(6), 1527.
[80] D. Abliz, Y. Duan, X. Zhao, D. Li, *Compos, Part A Appl. Sci. Manuf* **2014**, *65*, 73.
[81] A. Li, J. Fan, G. Li, *J. Mater. Chem. A* **2018**, *6*(24), 11479.
[82] S. Vasilakos, P. Tarantili, *J. Therm. Anal. Calorim.* **2017**, *127*(3), 2049.
[83] J. Menczel, R. Prime, *Thermal analysis of polymers: fundamentals and applications*, John Wiley & Sons, Hoboke **2009**.
[84] R. Hardis, J. L. P. Jessop, F. E. Peters, M. R. Kessler, *Compos, Part A Appl. Sci. Manuf.* **2013**, *49*, 100.
[85] V. Yuste-Sánchez, M. Hernández Santana, T. A. Ezquerra, R. Verdejo, M. A. López-Manchado, *Polym. Test.* **2019**, *80*, 106114.
[86] K. Hakala, R. Vatanparast, S. Li, C. Peinado, P. Bosch, F. Catalina, H. Lemmetyinen, *Macromolecules* **2000**, *33*(16), 5954.
[87] F. Lionetto, R. Rizzo, V. A. M. Luprano, A. Maffezzoli, *Mater. Sci. Eng., A* **2004**, *370*(1–2), 284.
[88] R. Lyon, K. Chike, S. Angel, *J. Appl. Polym. Sci.* **1994**, *53*(13), 1805.
[89] L. Merad, M. Cochez, S. Margueron, F. Jauchem, M. Ferriol, B. Benyoucef, P. Bourson, *Polym. Test.* **2009**, *28*(1), 42.
[90] B. Jang, W. Shih, *Mater. Manuf. Process* **1990**, *5*(2), 301.
[91] M. Włodarska, G. Bąk, B. Mossety-Leszczak, H. Galina, T. Pakula, *J. Non-Cryst. Solids* **2007**, *353*(47–51), 4371.
[92] S. D. Senturia, N. F. Sheppard, presented at Epoxy Resins Compos. IV. Massachusetts Inst of Tech Cambridge Center for Materials Science and Engineering, May 1–Oct 7, 1986. pp. 1–47.
[93] C. Y. Shigue, R. G. S. dosSantos, C. A. Baldan, E. Ruppert-Filho, *IEEE Trans. Appl. Supercond.* **2004**, *14*(2), 1173.
[94] R. Polanský, J. Pihera, J. Komárek, R. Pavlica, P. Prosr, J. Freisleben, R. Vik, K. Hromadka, T. Blecha, J. Čengery, R. Soukup, M. Čermák, M. Zemanová, P. Kadlec, A. Hamáček, *Compos Part A: Appl. Sci. Manuf.* **2016**, *90*, 760.
[95] F. Lionetto, F. Montagna, A. Maffezzoli, *Appl. Rheol.* **2005**, *15*(5), 326.
[96] F. Lionetto, A. Maffezzoli, *Materials* **2013**, *6*(9), 3783.
[97] M. Zhang, O. Bareille, M. Salvia, *Constr. Build. Mater.* **2019**, *225*, 196.
[98] C. Tuloup, W. Harizi, Z. Aboura, Y. Meyer, B. Ade, K. Khellil, *Mater. Today Commun.* **2020**, *24*, 101077.
[99] D. Chen, X. Zheng, *Sci. Rep.* **2018**, *8*(1), 1.
[100] C. Yan, X. Feng, C. Wick, A. Peters, G. Li, *Polymer* **2021**, *214*, 123351.
[101] G. X. Gu, C.-T. Chen, M. J. Buehler, *Extreme Mech. Lett.* **2018**, *18*, 19.
[102] G. X. Gu, C. T. Chen, D. J. Richmond, M. J. Buehler, *Mater. Horiz.* **2018**, *5*(5), 939.
[103] A. M. Mirzendehdel, K. Suresh, *Comput.-Aided Des.* **2016**, *81*, 1.
[104] H. Chi, Y. Zhang, T. L. E. Tang, L. Mirabella, L. Dalloro, L. Song, G. H. Paulino, *Comput. Methods Appl. Mech. Eng.* **2021**, *375*, 112739.

[105] S. Banga, H. Gehani, S. Bhilare, S. Patel, L. Kara, 3D topology optimization using convolutional neural networks. arXiv preprint arXiv:1808.07440, 2018.
[106] T. Zegard, G. H. Paulino, *Struct. Multidiscip. Optim.* **2016**, *53*(1), 175.
[107] M. Leary, L. Merli, F. Torti, M. Mazur, M. Brandt, *Mater. Des.* **2014**, *63*, 678.
[108] D. Brackett, I. Ashcroft, R. Hague, presented at Proc. Solid Freef. Fab. Symp. Austin, TX, 2011.
[109] A. T. Gaynor, N. A. Meisel, C. B. Williams, J. K. Guest presented at 15th AIAA/ISSMO Multidiscip. Anal. Opt. Conf. 2014.
[110] I. Sosnovik, I. Oseledets, *Russ. J. Numer. Anal. Math. Model.* **2019**, *34*(4), 215.
[111] S. S. Razvi, F. Shaw, N. Anantha, L. Yung-Tsun, W. Paul, presented at Int. Des. Eng. Tech. Conf. Comput. Inform. Eng Conf. American Society of Mechanical Engineers, 2019.
[112] A. Caggiano, J. Zhang, V. Alfieri, F. Caiazzo, R. Gao, R. Teti, *CIRP Ann.* **2019**, *68*(1), 451.
[113] L. Scime, J. Beuth, *Addit. Manuf.* **2018**, *19*, 114.
[114] Z. Jin, Z. Zhang, G. X. Gu, *Manuf. Lett.* **2019**, *22*, 11.
[115] K. Okarma, J. Fastowicz, Computer vision methods for non-destructive quality assessment in additive manufacturing. in *International Conference on Computer Recognition Systems*, Springer, **2019**, 11.
[116] D. J. Roach, A. Rohskopf, C. M. Hamel, W. D. Reinholtz, R. Bernstein, H. J. Qi, A. W. Cook, *Addit. Manuf.* **2021**, *41*, 101950.
[117] O. G. Kravchenko, C. Li, A. Strachan, S. G. Kravchenko, R. B. Pipes, *Compos, Part A Appl. Sci. Manuf.* **2014**, *66*, 35.
[118] L. Friedrich, M. Begley, In situ digital image analysis in direct ink writing. in *Polymer-Based Additive Manufacturing: Recent Developments*, ACS Publications, Switzerland **2019**, p. 131.
[119] Z. Li, Z. Zhang, J. Shi, D. Wu, *Rob. Comput. Integr. Manuf.* **2019**, *57*, 488.
[120] C. Li, A. Strachan, *Polymer* **2010**, *51*(25), 6058.
[121] M. F. Khan, A. Alam, M. A. Siddiqui, M. S. Alam, Y. Rafat, N. Salik, I. Al-Saidan, *Mater. Today:. Proc.* **2021**, *42*, 521.
[122] B. N. Narayanan, P. Nilesh, L. Gregory, K. Beigh, presented at Appl. Mach. Learn. International Society for Optics and Photonics. 2019.
[123] J. F. I. Nturambirwe, U. L. Opara, *Biosyst. Eng.* **2020**, *189*, 60.
[124] S. Chatterjee, S. Pouya, T. Schahin, K. Lutz, presented at ECIS, 2018.
[125] R. Li, M. Jin, V. C. Paquit, *Mater. Des.* **2021**, *206*, 109726.
[126] A. Sahu, A. Singh, S. Pandita, V. Walimbe, S. Kharche, Detection and correction of potholes using machine learning. in *Cybernetics, Cognition and Machine Learning Applications*, Springer, Switzerland, **2021**, p. 139.
[127] M. Ogunsanya, J. Isichei, S. K. Parupelli, S. Desai, Y. Cai, *Procedia Manuf.* **2021**, *53*, 427.
[128] H. Zhang, M. Seung, N. Teck, T. Junjie, M. Ashrof, presented at 2018 Int. Conf. Intell. Rail Transp. IEEE, 2018.

How to cite this article: C. Gao, J. Qiu, S. Wang, *J. Adv. Manuf. Process.* **2022**, *4*(3), e10114. https://doi.org/10.1002/amp2.10114